AUTHOR'S COPY:

Endoscopic Stone Measurement During Ureteroscopy

Wesley W. Ludwig[1], Sunghwan Lim[2], Dan Stoianovici[12], Brian R. Matlaga[1]

Affiliations: [1]The James Buchanan Brady Department of Urology, [2]Robotics Laboratory, School of Medicine, Johns Hopkins University

Authors address:

The James Buchanan Brady Urological Institute and Department of Urology

The Johns Hopkins University School of Medicine

600 North Wolfe Street | Marburg 134

Baltimore, MD 21287

Email addresses:

Wesley W. Ludwig: wludwig1@jhmi.edu

Sunghwan Lim: shjlim@jhu.edu

Dan Stoianovici: dss@jhu.edu

Corresponding Author: Brian R. Matlaga: bmatlag1@jhmi.edu

Running Title: Stone measurement during URS

Keywords: Stone measurement, flexible ureteroscopy, nephrolithiasis

Word count:

Abstract

Introduction: Currently, stone size cannot be accurately measured while performing flexible ureteroscopy (URS). We developed novel software for ureteroscopic, stone size measurement, and then evaluated its performance.

Methods: A novel application capable of measuring stone fragment size, based on the known distance of the basket tip in the ureteroscope's visual field, was designed and calibrated in a laboratory setting. Complete URS procedures were recorded and 30 stone fragments were extracted and measured using digital calipers. The novel software program was applied to the recorded URS footage in order to obtain ureteroscope-derived stone size measurements. These ureteroscope-derived measurements were then compared to the actual measured fragment size.

Results: The median longitudinal and transversal error was 0.14 mm (95%CI 0.1-0.18) and 0.09 mm (95%CI 0.02-0.15), respectively. The overall software accuracy and precision were 0.17 mm and 0.15 mm, respectively. The longitudinal and transversal measurements obtained by the software and digital calipers were highly correlated (r = 0.97 and 0.93). Neither stone size nor stone type was correlated with error measurements.

Conclusions: This novel method and software reliably measured stone fragment size during URS. The software ultimately has the potential to make ureteroscopy safer and more efficient.

Introduction

Urolithiasis is becoming increasingly prevalent, and flexible ureteroscopy (URS) is a very common treatment modality.[1,2] URS provides an acceptable stone free rate and utilization of this technique has been increasing at a great rate.[3,4] A common challenge during URS is accurately determining the size of a visualized object. To this end, urologists often use some combination of either comparison to known landmarks or reference to implements of a known size in order to estimate stone dimensions. However, this can be an unreliable metric, particularly for individuals who are less familiar with URS. Currently, there is no purpose-built tool to measure stone size during URS.

The ability to measure stone fragment size is particularly important for intraoperative decision-making. An accurate size measurement determines the need for and extent of further fragmentation, likelihood of spontaneous fragment passage, and ability to safely extract fragments through a ureter or ureteral access sheath. Additionally, underestimation of stone fragment size can lead to complications such as ureteral trauma or an entrapped basket.[5,6] Misjudging stone size can also result in multiple exchanges of ureteroscopic instruments and discontinuous stone fragmentation which can increase operative time and decrease surgeon productivity.

To achieve an accurate and objective quantification of stone fragment size we developed novel software that performs intraoperative measurement of objects during URS. The software was utilized in recorded video from URS procedures for ureteral and renal stones during basket extraction of fragments. We tested the software's accuracy and precision with stone fragments of varying sizes in order to determine the feasibility and performance of this technology.

Methods:

The size of an object viewed through a ureteroscope depends on its distance from the end of the scope. Distance can be estimated by the length of wire advancement when touching a target object and depth can be measured from the ureteroscopic image. A geometric model, calibration procedure, and software tool were developed to implement this method.

a) Geometric Model: Object size as viewed in an image is inversely related to its distance from the ureteroscope tip. Size determination as related to the depth of the wire measured in the actual image was calculated using mathematics described in supplemental figure 1. This dependency was then used for the experimental calibration of the image scale, followed by actual stone measurements.

Ureteroscopes typically include a wire channel on the side. A checkerboard calibration rig is placed in front of the scope and the distance between the side of the wire and the optical axis was determined. During insertion through the scope, the wire is not initially visible in the image. When advanced deeper, the tip of the wire exits the scope and appears on the side of the image. In the image the wire appears to advance laterally, from the edge towards the center of the image, therefore depth is measured laterally (supplemental figure 2).

b) Calibration: A single-use ureteroscope (Lithovue, Boston Scientific) and a guide-wire (Ø0.965mm, Hydro-Glide, Bard) were used. The end of the ureteroscope was fixed on a testing device. A checkerboard (8x6 mm) was mounted to a linear sliding stage aligned with the optical axis of the scope. Ureteroscopic images were acquired with a video capture device (AV.io HD, Epiphan Systems, Canada) from the DVI output of the ureteroscope.

Endoscopic images are typically radially distorted; thus, the first step of calibration is image dewarping. Distortion correction was performed with a common technique [13]. In short, warping was measured based on checkerboard images, and a reverse transformation was applied to dewarp the image. Dewarping is then applied in real-time to the images acquired. The entire calibration was repeated with a second ureteroscope of the same kind, to compare the results. Total calibration time was under five minutes.

c) Measurement: The calibration coefficients were used to measure the size of objects (stones) in the image: 1) a wire or instrument was advanced to the object, 2) the size and depth of the object in the image was calculated.

d) Software was developed in Visual Studio 2017 (C++, Microsoft Corp.) with open source computer vision library (OpenCV). The software implemented the distortion correction and measurement methods described above. A scale was represented on the sides of the image as shown in Figure 1(b, d) that changes according to the depth.

e) Study: In an IRB-approved study URS was performed for ureteral and renal stones per standard of care in five patients over the age of 18 without identified genitourinary abnormality. A new single-use digital ureteroscope of the same model employed for the calibration was used in each case. Stones were fragmented with a 200-micron laser fiber and a 1.9 French Zero Tip nitinol stone retrieval basket (Boston Scientific) was used for stone extraction. Recordings were obtained throughout the duration of each ureteroscopic case - starting with rigid cystoscope insertion and terminating with ureteral stent placement. A ureteral access sheath (Navigator HD, 11/13 French, Boston Scientific) was used in one case in which numerous renal stones were present. Immediately following extraction, fragments were numbered and digital calipers (Mitutoyo CD-8”CSX, Japan) were used to measure the longitudinal (S_l) and transversal (S_t) axes of the stone, as shown in Figure 1(a, c). Caliper measurement provided the gold-standard measurement for comparison to the software-acquired stone measurements.

Recorded images were analyzed after the procedure. The size of the stone from the images was measured while the stone fragment was within the endoscopic basket, as shown in Figure 1(b, d) and the entire stone and basket were visible. Stone measurement can occur with any fragment that is in close proximity to a ureteroscopic instrument that has undergone previous calibrations. The workflow of the software program requires that the user select a portion of the basket in contact with the stone to measure depth and calibrate the image scale. This scale then becomes visible around the periphery of the

image and can be used for future measurement reference, as seen in Figure 1(b, d) Following this, measurements can either be performed using the visible scale or selection of the object sides. The longitudinal (s_l) and transversal (s_t) sizes of the stone were measured for all stones. Figure 2 shows the linear regression results of the ureteroscopes. The two constant parameters, are $R_1 = 1.135\,[\mathrm{mm}]$ and $r_1 = 501\,[\mathrm{pixel}]$ for Scope 1 and $R_2 = 1.115\,[\mathrm{mm}]$ and $r_2 = 508.2\,[\mathrm{pixel}]$ for Scope 2. Their respective average parameters are $R = 1.125\,[\mathrm{mm}]$ and $r = 504.6\,[\mathrm{pixel}]$. These values were used in the measurements. The time to measure fragments was equivalent to time to caliper placement.

Measurement errors were calculated as the difference between the software and caliper measured sizes in mm, for both the longitudinal and transversal measurements. The accuracy and precision of measurements were calculated as the average and standard deviation of the errors over the entire dataset, as usual. Additionally, confidence intervals and Pearson's correlation coefficients were calculated for corresponding measurements. Analyses were performed using R version 3.1.2. A p-value <0.05 was considered statistically significant.

Results

URS was performed for 18 stones in five patients, which resulted in 30 measured stone fragments (See Figure 3), and 60 longitudinal and transversal measurements. Patient and stone characteristics can be seen in Table 1. The pre-operative median stone size was 3.0±2.0 mm, with the largest stone measuring 8.0 mm. All stone fragments saved for analysis could be measured and no technical difficulties were encountered with this task. The longitudinal and transversal stone fragment measurements obtained by software and caliper measurement are listed in Table 2. The median longitudinal and transversal stone fragment size as measured by digital calipers were 3.2±0.8 mm and 2.2±0.6 mm, respectively. The median longitudinal and transversal stone fragment size measurements determined by the software were 3.2±0.8 mm and 2.0±0.6 mm, respectively. The median longitudinal and transversal error was 0.14 mm (95%CI 0.1-0.18) and 0.09 mm (95%CI

0.02-0.15), respectively. The maximum errors measured for longitudinal and transversal measurements were 0.53 and 0.59 and the minimum measured were 0.02 and 0.01 mm.

The longitudinal and transversal accuracy of measurement were 0.17 and 0.17 mm, for an overall accuracy of 0.17 mm. The longitudinal and transversal precision to measure stone fragments were 0.12 and 0.18 mm, for an overall precision of 0.15 mm. The longitudinal and transversal measurements obtained by the software and digital calipers were highly correlated ($r = 0.97$ and 0.93, respectively). Stone size was not correlated with longitudinal and transversal error measurement ($r = 0.3$ and 0.1, respectively). Additionally, there were no statistically significant differences between errors measured in calcium oxalate and cystine stones ($p=0.2$).

Discussion:

We investigated the ability of a novel software application to measure stone fragments during URS. The software proved to be accurate and precise, with a median error less than 0.15 mm. Software measurements were highly correlated with standard measurement using digital calipers and there was no correlation between stone fragment size and error measured. Thus, this software can be used with a high degree of reliability, accuracy and precision during URS.

A limitation of the study was that the calibration was only performed with two scopes. Based on the accurate measurements performed with 4 other scopes it appears that the calibration coefficients are relatively constant. Since calibrating the actual single-use scope before the case is not feasible, one has to relay on previously derived calibration results, and scopes should have uniform characteristics. Testing a larger number of scopes and possibly setting uniform calibration characteristic among other manufacturing controls of the scopes would be helpful. In our study, we employed single-use ureteroscopes. The calibration and measurement methods, however, are readily applicable to reusable ureteroscopes and other types of scopes. In case of reusable scopes, it is possible to perform the calibration individually, if needed.

In our method and experiments the depth of the wire was estimated based on the view of the visible part of the wire in the images. The stone dimensions are simply marked with two reference points and a calculated size is provided. Thus, the amount of time for a urologist to calculate a particular stones size is negligible. The advantage of this approach is that it did not require additional hardware. An alternative approach is to employ a wire tracking device, such as a wire roller or spool, that could measure the depth of the wire tip in real time, to adjust the scale of the images in the plane of the wire point.

The ability to determine stone size during URS is both clinically relevant and commonly useful. An application of this technology is in assisting the determination of fragmentation completeness. While we used a basket to measure stone size, this same technology could be easily applied to any ureteroscopic instrument including lasers or wires. This is particularly true as the “dusting” technique is increasingly used in URS. Dusting relies on laser settings of a high frequency and low energy; this will fragment the stone into small pieces, or “dust”, which are then spontaneously discharged from the kidney.[7,8] However, without an accurate measure of fragment size, assumptions about stone passage may be erroneous. At other points during URS, particularly during basket extraction of fragments, stone size estimation is also required. Attempting to basket a particularly large stone can lead to stone impaction, necessitating multiple additional manipulations and significant case prolongation.[9,10] Importantly, attempting to remove a larger than anticipated stone can lead to substantial ureteral complications, including; injury, intussusception and avulsion.[6] Severe ureteral injuries often require reconstructive procedures and are associated with major morbidities and changes in quality of life.[11,12] Understanding stone fragment size can also potentially decrease operative time, as extraction would commence only once all fragments were small enough to be effectively removed.

While this technology is novel within the field of ureteroscopy, there have been previous attempts to create accurate endoscopic measurement tools- particularly in the field of gastroenterology.[13,14] However, these studies approached the problem in different manners. Vakil et al. designed software capable of obtaining endoscopic measurements, but it necessitated obtaining the distance between the tip of the scope and the object

which was measured using a guide wire with gradations.[13] Following calibration, the measurements in our study could be obtained without needing a new measure of distance for each stone measurement. Additional studies have also fallen short – allowing only measurement of luminal deformation[15], or simply permit a ruler-like adjunct to an endoscope.[14]

A limitation of the current study is that it was performed on URS video footage, as opposed to occurring in real-time. This was performed to determine the safety, feasibility, and accuracy of the measurement, prior to intraoperative measurement trials to follow. Additionally, stones are often complex shapes and transverse and longitudinal dimensions may differ somewhat between measurements obtained with calipers and software. Although rare, some fragment measurements had greater levels of error- up to 0.5 mm of inaccuracy. This could lead to an occasional imprecise measurement, but it remains to be determined if that is clinically relevant. Future studies will attempt to determine causative or predictive factors of stone measurement error. A foreseeable cause is the relative position of touching the stone with the wire, that may require clinical training.

Our current study represents an initial report of a novel application, with further studies planned to transition this technology to intraoperative use. Once this application can be utilized concurrently with existing endoscopic video equipment, an evaluation of its broader intraoperative performance will be undertaken. While we only measured stones while basketing, measurements can also be performed using other endoscopic instruments. Future studies will investigate measurements obtained using laser fibers or other ureteroscopic instruments to confirm similar results. Additional ureteroscope types, such as the more commonly used reusable fiber-optic and digital ureteroscopes will also be tested to confirm that accuracy and precision is maintained across ureteroscope type.

Conclusions:

This study describes a novel method and software application to measure the stone fragment size during URS. To the best of our knowledge, no mono-vision scope medical system provides the ability to measure objects in the image. Theoretically, the

measurements require stereo-vision for depth triangulation. However, we observed, demonstrated mathematically, and verified experimentally that the mono-vision measurement is possible with the help or a wire or other instrument advanced to the object, that is used as a surrogate of the missing depth information.

The accuracy and precision of the software were less than 0.19 mm, and the measurements between the software and digital calipers were highly correlated. The software's ease of use may permit its application to other types of endoscopy. Indeed, this could prove to be a useful tool for measuring not only stones, but also findings during cystoscopy, colonoscopy or laryngoscopy/bronchoscopy. Accurate and precise real-time endoscopic measurements would be of benefit to the entire medical community.

References

1. Scales, C. D., Smith, A. C., Hanley, J. M. & Saigal, C. S. Prevalence of kidney stones in the United States. *Eur. Urol.* **62,** 160–165 (2012).

2. Oberlin, D. T., Flum, A. S., Bachrach, L., Matulewicz, R. S. & Flury, S. C. Contemporary surgical trends in the management of upper tract calculi. *J. Urol.* **193,** 880–884 (2015).

3. Geraghty, R., Jones, P. & Somani, B. Worldwide Trends of Urinary Stone Disease Treatment over the last two Decades: A Systematic Review. *J. Endourol.* **Jan,** doi: 10.1089/end.2016.0895. [Epub ahead of print] (2017).

4. de la Rosette, J. *et al.* The clinical research office of the endourological society ureteroscopy global study: indications, complications, and outcomes in 11,885 patients. *J. Endourol.* **28,** 131–9 (2014).

5. Teichman, J. M. & Kamerer, A. D. Use of the holmium:YAG laser for the impacted stone basket. *J. Urol.* **164,** 1602–1603 (2000).

6. de la Rosette, J. J. M. C. H., Skrekas, T. & Segura, J. W. Handling and Prevention of Complications in Stone Basketing. *European Urology* **50,** 991–999 (2006).

7. Chawla, S. N., Chang, M. F., Chang, A., Lenoir, J. & Bagley, D. H. Effectiveness of High-Frequency Holmium:YAG Laser Stone Fragmentation: The 'Popcorn Effect'. *J. Endourol.* **22,** 645–650 (2008).

8. Emiliani, E. *et al.* Optimal Settings for the Noncontact Holmium-YAG Stone Fragmentation Popcorn Technique. *J. Urol.* **23,** 57750–2 (2017).

9. Allen, D., Hindley, R. & Glass, J. Baskets in the kidney: an old problem in a new situation. *J. Endourol.* **17,** 495–6 (2003).

10. Ansari, M. S., Goel, A., Karan, S. C. & Aron, M. Holmium: YAG laser rescue for a stuck stone basket. *Int. Urol. Nephrol.* **34,** 463–464 (2002).

11. Tanimoto, R., Cleary, R., Bagley, D. & Hubosky, S. Ureteral Avulsion Associated with

Ureteroscopy: Insights from the MAUDE Database. *J. Endourol.* **30,** 257–61 (2016).

12. Ge, C. *et al.* Management of complete ureteral avulsion and literature review: a report on four cases. *J. Endourol.* **25,** 323–326 (2011).

13. Vakil, N., Smith, W., Bourgeois, K., Everbach, E. & Knyrim, K. Endoscopic measurement of lesion size: improved accuracy with image processing. *Gastrointest. Endosc.* **40,** 178–83 (1994).

14. Kume, K., Wattanabe, T., Yoshikawa, I. & Harada, M. Endoscopic measurement of polyp size using a novel calibrated hood. *Gastroenterol. Res. Pract.* **2014,** 714294 (2014).

15. Matthys, D., Gilbert, J. & Greguss, P. Endoscopic measurement using radial metrology with digital correlation. *Opt. Eng.* **30,** (1991).

13. Z. Zhang, “A Flexible New Technique for Camera Calibration,” IEEE Transaction on Pattern Analysis and Machine Intelligence, vol. 20, no. 11, 2000.

Abbreviations:

URS- ureteroscopy

Table 1. Longitudinal and transversal measurements for each stone fragment as measured by digital calipers and software, with listed errors. All measurements in mm.

Age (median)	61±18.2
Sex	Male: 5 (100%)
BMI	23.1±3.1
Race	Caucasian: 5 (100%)
History of previous URS	2 (40%)
Side	Left: 2 (40%)
	Right: 2 (40%)
	Bilateral: 1 (20%)
Location	Ureteral: 2 (40%)
	Renal: 3 (60%)
Pre-op stone measurement (median ± std dev)	3.0 ± 2.1 mm
Pre-stented	2 (40%)
Ureteral access sheath used	1 (20%)
Stone composition	Calcium oxalate: 4 (80%)
	Cystine: 1 (20%)

Table 2. Longitudinal and transversal measurements for each stone fragment as measured by digital calipers and software, with listed errors. All measurements in mm.

Fragment #	Distance d [pixel]	Longitudinal [mm]			Transversal [mm]		
		Caliper	Software	Error	Caliper	Software	Error
1	343	3.98	4.03	0.05	3.32	3.38	0.06
2	373	4.18	4.11	0.07	2.20	1.82	0.38
3	266	1.49	1.55	0.06	1.22	1.28	0.06
4	326	2.39	2.65	0.26	1.78	1.79	0.01
5	331	1.95	2.17	0.22	1.63	1.59	0.04
6	396	3.86	3.76	0.10	2.56	2.63	0.07
7	250	3.66	3.33	0.33	1.92	1.81	0.11
8	299	3.76	3.23	0.53	2.19	1.80	0.39
9	247	3.14	2.95	0.19	1.67	1.73	0.06
10	362	3.52	3.22	0.30	2.54	2.58	0.04
11	315	2.23	2.37	0.14	1.74	1.17	0.57
12	342	3.64	3.54	0.10	3.05	2.97	0.08
13	402	4.15	4.44	0.29	2.74	3.28	0.54
14	291	2.63	2.68	0.05	2.08	1.90	0.18
15	125	3.23	3.37	0.14	3.21	3.09	0.12
16	310	2.58	2.35	0.23	1.48	1.44	0.04
17	315	3.63	3.71	0.08	2.34	2.53	0.19
18	302	2.50	2.19	0.31	1.05	1.02	0.03
19	390	4.03	3.69	0.34	2.38	2.48	0.10
20	365	4.84	4.52	0.32	2.94	2.88	0.06
21	240	1.91	1.93	0.02	1.58	1.51	0.07
22	348	2.92	2.75	0.17	1.96	1.89	0.07
23	272	3.22	3.17	0.05	2.40	2.49	0.09
24	318	2.45	2.39	0.06	2.22	1.63	0.59
25	402	3.88	3.79	0.09	2.06	2.28	0.22

26	254	2.43	2.33	0.10	2.30	1.82	0.48
27	273	2.91	2.05	0.12	2.79	2.11	0.06
28	418	4.09	2.44	0.10	4.19	2.23	0.21
29	328	2.93	2.24	0.18	2.75	2.18	0.06
30	335	3.20	2.90	0.22	3.42	2.75	0.15

Figure legends:

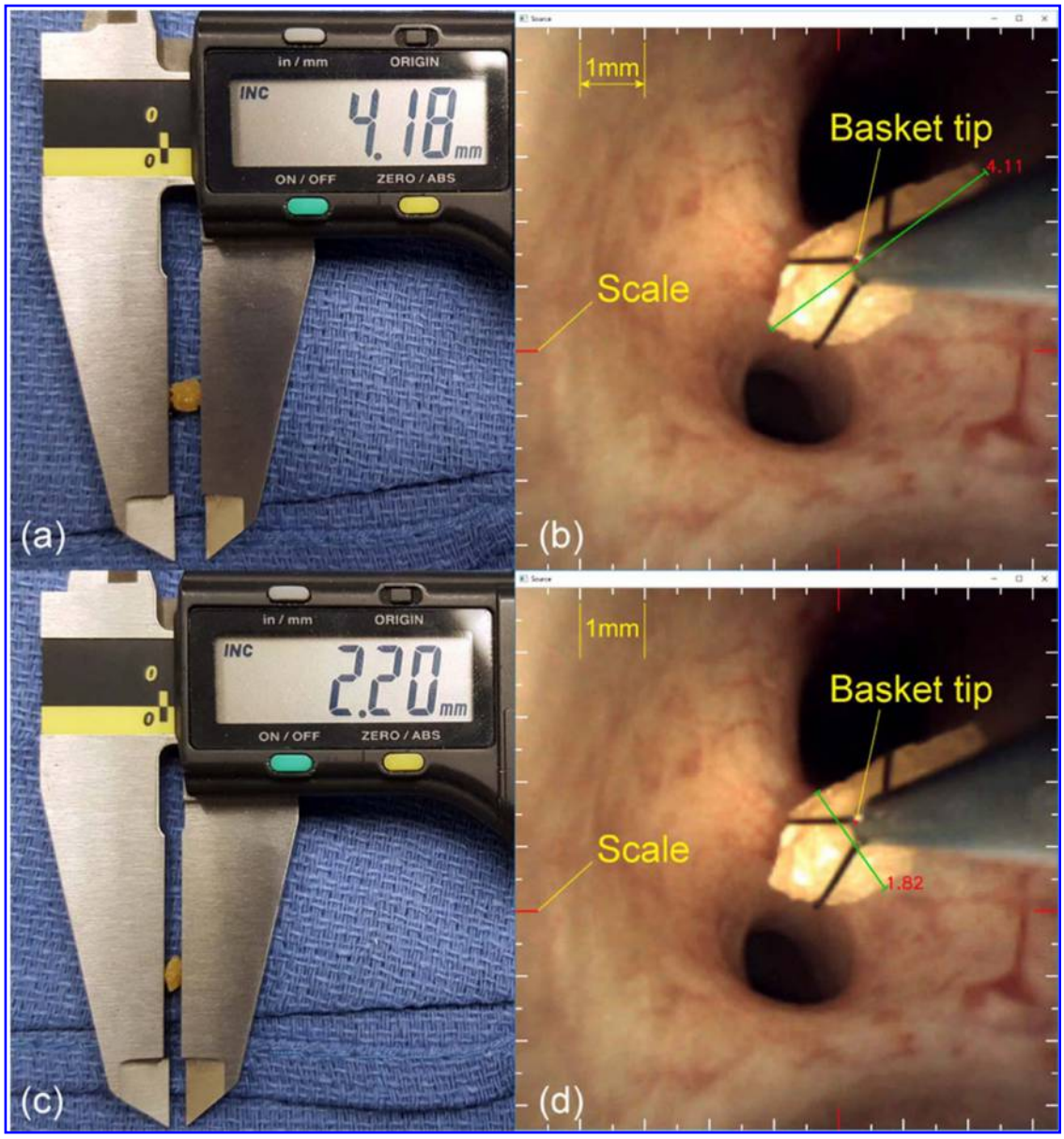

Figure 1. Method of stone measurement. (a, c) Stone fragment as measured by digital calipers. (b, d) The same stone as measured by software. The fragment is grasped within the basket and the basket tip serves as the reference point for stone measurement. A scale can be seen around the periphery of the image, with a 1 mm measurement marked in yellow. Stone can also be measured by selecting the limits of the stone (seen in green, with corresponding stone measurement of 4.11 and 1.82 mm).

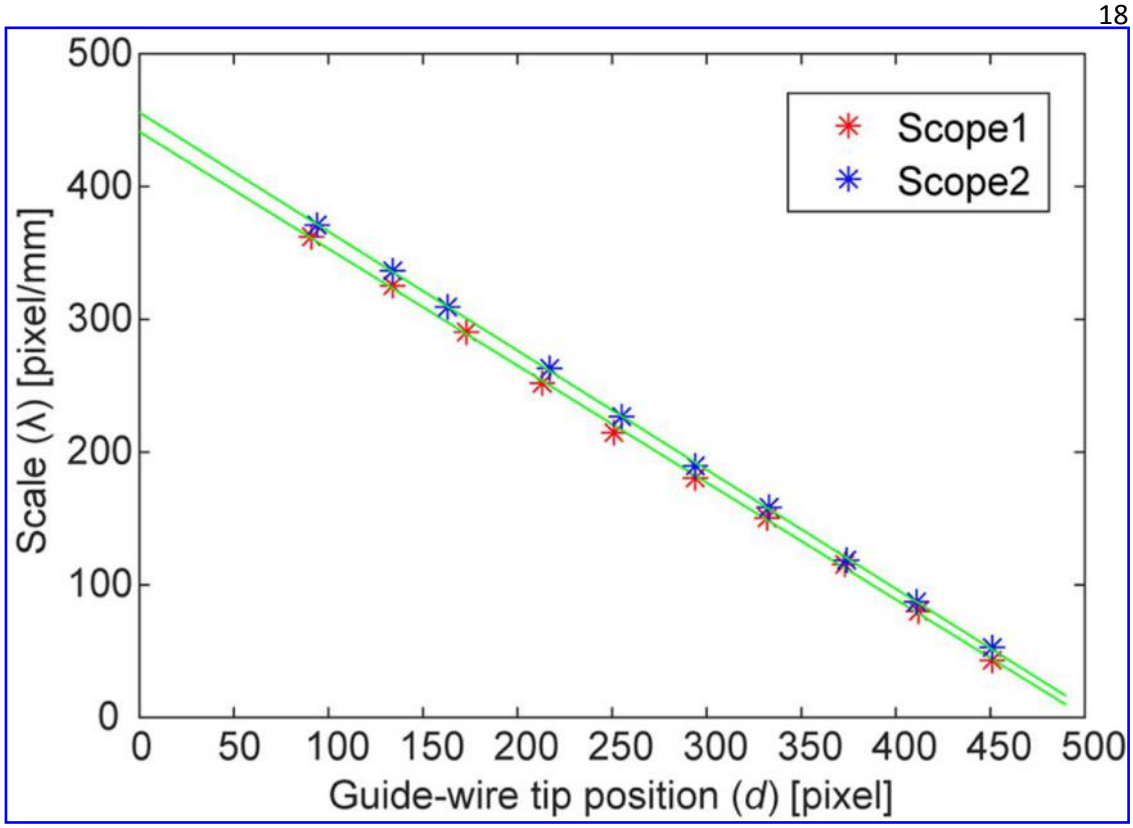

Figure 2. Calibration results of two ureteroscopes. Red and blue asterisks indicate measurement values of the scopes. Green lines indicate linear regression results.

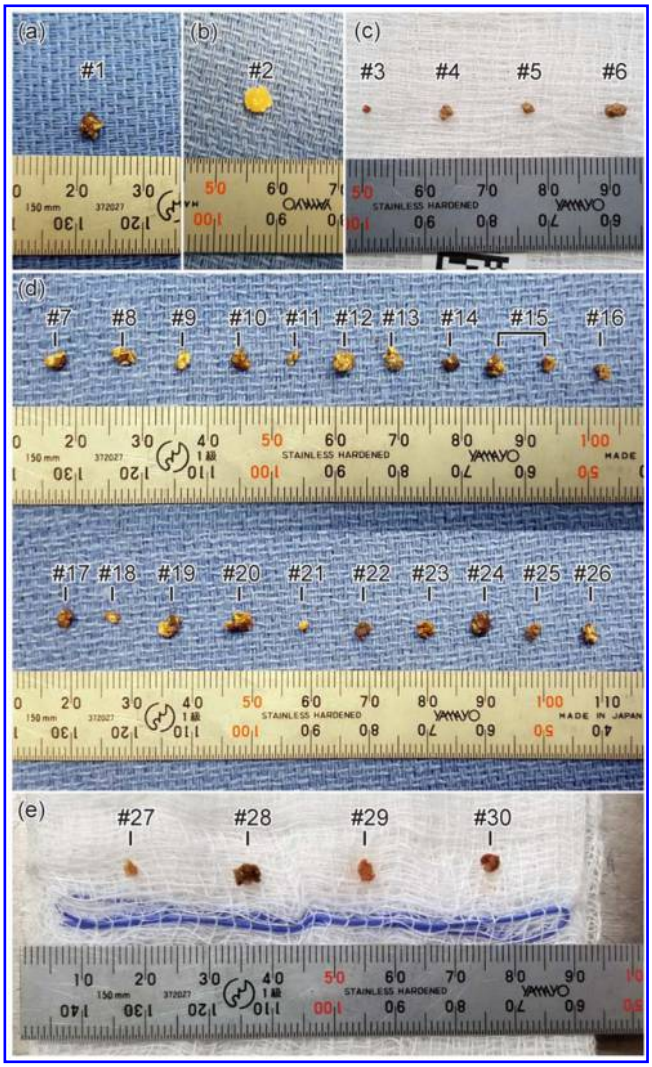

Figure 3. Stone fragments from (a) patient 1, (b) patient 2, (c) patient 3, and (d) patient 4.

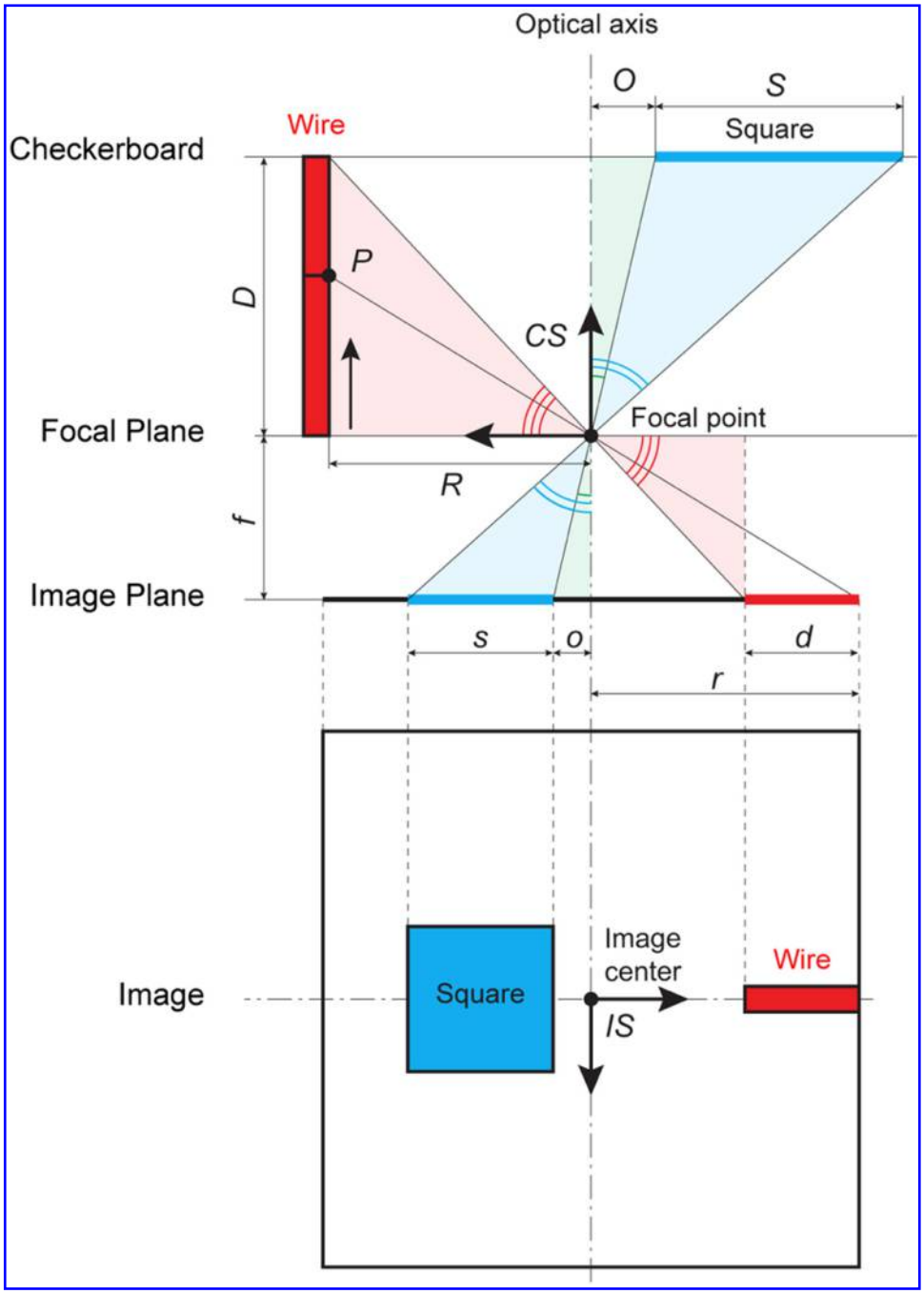

Supplemental Figure 1. Displays a schematic of measurement principle. The physical space (camera space, CS) at the top side and the image space (IS) at the bottom. A square of the board having the size S [mm] and the horizontal offset of O [mm] is shown, at a distance D [mm] from the focal plane. The si are variables and other are constant parameters.

$$\frac{O}{o} = \frac{D}{f} \Rightarrow o = O\frac{f}{D} \quad (1)$$

$$\frac{O+S}{o+s} = \frac{D}{f} \Rightarrow s = (O+S)\frac{f}{D} - o = S\frac{f}{D} \quad (2)$$

$$\frac{D}{f} = \frac{R}{r-d} \Rightarrow D = \frac{Rf}{r-d} \quad (3)$$

By substution,

$$s = S\frac{r-d}{R} = \left(-\frac{S}{R}\right)d + \frac{Sr}{R} \quad (4)$$

The scale of the image λ [pixel/mm] is,

$$\lambda = \frac{s}{S} = \left(-\frac{1}{R}\right)d + \frac{r}{R} \quad (5)$$

This shows that the scale of the objects in the image (λ) is inversely related $\left(-\frac{1}{R}\right)$ to the depth to the object measured in the image (d), with an offset $\left(\frac{r}{R}\right)$.

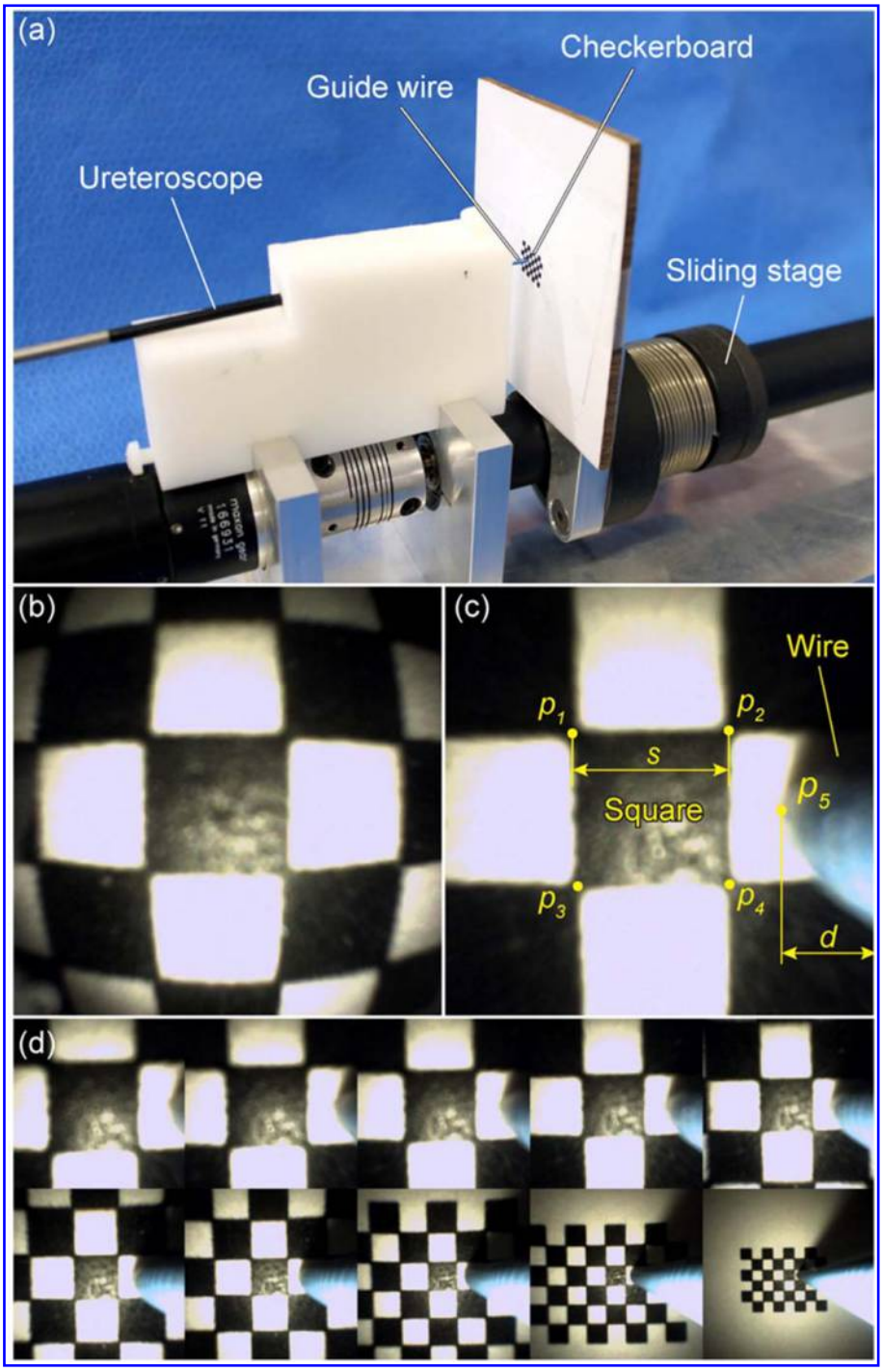

Supplemental Figure 2. Ureteroscope calibration; (a) experimental setup, (b) original ureteroscopic image (distorted), (c) processed image (undistorted), and (d) checkerboard images captured at different positions. The checkerboard was translated to 10 locations ($D_i, i = 1 - 10$), and its images were captured at each position, as shown in Figure 2(d).